SPECIAL ISSUE: Celebrating the 100th Anniversary of Nankai University

Fe/Co-based nanoparticles encapsulated in heteroatom-doped carbon electrocatalysts for oxygen reduction reaction

Baoxia Ni, Luming Wu, Rui Chen, Chengxiang Shi and Tiehong Chen[*]

ABSTRACT It is crucial to develop low-cost and highly efficient catalysts for oxygen reduction reaction (ORR) which is the key process in electrochemical energy conversion and storage devices. Transition metal-based nanoparticles/carbon materials are an important class of non-noble metal catalysts that have attracted considerable research interest. The topic of this review is mainly focused on carbon encapsulated Fe/Co-based nanoparticles catalysts for ORR, and these catalysts are summarized in categories of metals, oxides, carbides, phosphides, sulfides and hybrid nanoparticles. The structures and morphologies of the carbon matrix as well as compositions of nanoparticles have great influence on the catalytic performance. Numerous catalysts display excellent ORR activity and stability in alkaline media but only a few are efficient in acidic media. In addition, challenges and further strategies on the development of this type of carbon encapsulated nanoparticles catalysts are also proposed.

Keywords: Fe/Co based nanoparticles, encapsulation, carbon, oxygen reduction reaction

INTRODUCTION

In the past decades, energy crisis and environmental pollution have been serious issues due to the development of industry. Therefore, the environment-friendly energy devices such as fuel cells and metal-air batteries have attracted significant attention [1]. At present, the sluggish kinetics of oxygen reduction reaction (ORR) hinders the widespread application of these energy conversion and storage devices [2]. Up to now, the most efficient catalysts for ORR are platinum-based electrocatalysts, but they suffer from scarce reserve, high cost, poor stability and tolerance to CO and methanol [3]. Many efforts have been made to explore non-precious-metal (NPM) catalysts and numerous publications have been reported on the design and synthesis of catalysts for ORR [4–5]. Among various NPM catalysts, modified carbon materials have emerged as promising candidates due to the excellent electrical conductivity and large specific surface area. Currently, single or multiple non-metal atoms (e.g., B, N, S and P) and non-precious metal atoms (e.g., Fe, Co, Ni) were doped into carbon materials [6–12], and both experimental results and density functional theory (DFT) calculations have revealed that the incorporation of heteroatoms could modify the intrinsic charge distribution of carbon and reduce the energy barrier of oxygen adsorption, and thus improve the ORR activity of catalysts [13–18].

Metal-based nanoparticles (NPs) were often generated by an annealing process [19–23], and significant progress in metal-based NPs encapsulated within heteroatom-doped carbon catalysts for ORR has been reported [24]. During the annealing process, metal or other heteroatoms were doped into carbon matrix, and metal-based NPs were encapsulated by heteroatom-doped carbon layers. This encapsulation configuration has been studied in-depth by Deng and co-workers [25], and it was proposed that the confined metal NPs could decrease the local work function on the carbon surface through electron transfer, leading to the enhanced catalytic activity. The carbon layers also protected metal NPs from directly contacting with harsh environments (electrolytes, oxygen or other molecules), leading to excellent long-term stability. This type of electron interaction between the encapsulated NPs

---

Institute of New Catalytic Materials Science, School of Materials Science and Engineering, Key Laboratory of Advanced Energy Materials Chemistry (MOE), Nankai University, Tianjin 300350, China
[*] Corresponding author (email: chenth@nankai.edu.cn)

and coating carbon layers appeared in many reported catalysts, and due to the diversity of NP species and porous carbon structures, multiple carbon-encapsulated NP electrocatalysts for ORR have been fabricated. The structure and porosity of carbon matrix could affect mass transport, electron transfer and exposure of active sites [26,27], and therefore the design of carbon materials with hierarchically porous structures is beneficial to efficient oxygen reduction process. In addition, NP species, sizes and distribution are also crucial factors that influence the synergistic effect between heteroatom-doped carbon layers and encapsulated NPs, and improving the dispersity of fine NPs is an effective strategy to create uniformly distributed active sites.

Diverse precursors and approaches have been reported to prepare catalysts with carbon-encapsulation structure. In this review, the topic is mainly focused on the recent progress in heteroatom-doped carbon catalysts with encapsulated Fe/Co-based NPs for ORR. In order to identify the role of NP species, these catalysts are summarized in categories according to the type of encapsulated NPs in six parts: Fe/Co metals, carbides, phosphides, oxides, sulfides and hybrid NPs. The effects of morphologies, carbon structures, NP species and other factors are discussed, and the ORR performances of these catalysts are listed and compared. Finally, challenges and perspectives of this rapidly growing field are proposed.

CARBON ELECTROCATALYSTS DECORATED WITH Fe/Co BASED NPs

In this section, synthesis methods and ORR activities of catalysts were discussed. Most of the reported NPs/carbon catalysts were efficient in alkaline media, but a few were efficient in acidic media (summarized in Tables 1 and 2). These encapsulation catalysts displayed excellent catalytic stability and methanol tolerance compared with platinum-based catalysts.

Fe/Co metal NPs

Varnell and co-workers [28] reported a remarkable research to reveal the active sites responsible for ORR activities. In their study, the catalysts containing carbon-coated Fe particles and Fe-N species were treated by Cl_2 and H_2 at high temperature, respectively (shown in Fig. 1). Through characterization of the deactivated and reactivated catalysts, it was revealed that Fe-N species were not essential for ORR, while the Fe particles coated by N-doped carbon layers were responsible for the active ORR activity. Hence, the positive effect of N-doped carbon coated Fe NPs was proved. Strickland et al. [29]

proposed that the electron transfer from Fe NPs to the N-doped carbon shell contributed to the efficient ORR performance, indicating that both Fe NPs and N doping in carbon shell were crucial for the improved ORR activity.

Metal-organic frameworks (MOFs) have attracted great interest due to their diverse compositions and ordered structures. Fe/Co encapsulated catalysts were largely fabricated with MOFs as precursors. For example, the pyrolysis of iron-based MIL-100 generated Fe particles, which catalyzed surrounding carbon atoms to form graphitic carbon layers [30]. N-doped porous carbon with Co NP-embedded carbon nanotubes (CNTs) (Co-CNT/PC) was prepared by annealing ZIF-67 with encapsulated Co_3O_4. The preloaded Co_3O_4 NPs catalyzed CNTs growth and ZIF-67 was transformed into N-doped porous carbon [31]. Li et al. [32] designed a novel approach to prepare N-doped CNTs decorated with carbon-coated cobalt NPs with ZIF-67 as precursor. The outer surface of halloysite nanotubes (HNTs) with negative charge tended to adsorb Co^{2+}, inducing the growth of ZIF-67 on the surface. After pyrolysis and etching process, the resulting catalyst with large surface area and hollow nanotube structure was obtained. Hybrid ZIF-67 with regulated Zn/Co ratio was explored by in-situ growth on the g-C_3N_4 nanosheets, and the obtained carbon materials were closely related to the Zn/Co ratio of precursors (shown in Fig. 2). The one-dimensional (1D) bamboo-like carbon nanotubes were highly efficient for ORR compared with two-dimensional (2D) nanosheets and three-dimensional (3D) CNT-framework, indicating the important role of carbon structure on ORR performances [33]. Annealing the mixture of cobalt salt and g-C_3N_4 could obtain an efficient bifunctional electrocatalyst with a tetragonal microscopic structure [34].

N-heterocyclic carbene-Co complex was applied as the precursor to prepare Co NPs/carbon catalysts without metal-nitrogen bonding [35]. Based on experimental results, the ORR activity was contributed from the C-N sites surrounding Co NPs. The DFT calculations further demonstrated that the electron transfer from Co NPs to the N-doped carbon layers resulted in charge redistribution and decreased local work function on the outer carbon surface. While, Zeng and co-workers [36] proposed the Co-N-C moieties were active sites and the inner Co cores were not effective for ORR activities. However, it was reported that FeCo alloy NPs encapsulated in N-doped carbon were also active for ORR [37,38].

Taking the commercial application into account, the ORR performance in acidic media and the long-term

Table 1 Comparision of ORR performances of Fe/Co-based NPs carbon catalysts in alkaline media

Samples	E_{onset} (V)	$\triangle E_{onset}$ (mV)	$E_{1/2}$ (V)	$\triangle E_{1/2}$ (mV)	Ref.
Co@C-NCNTs	−0.104 (*vs.* Ag/AgCl)	−60	−0.162 (*vs.* Ag/AgCl)	−28	[32]
Co/N-BCNTs	-	-	0.83 (*vs.* RHE)	10	[33]
Co-N-C-0.4	0.98 (*vs.* RHE)	0	0.84 (*vs.* RHE)	0	[34]
Co-NHC-900	-	-	0.85 (*vs.* RHE)	10	[35]
FeCo@MNC	-	-	0.86 (*vs.* RHE)	10	[37]
Fe@C_2N	1.015 (*vs.* RHE)	−6	0.876 (*vs.* RHE)	32	[40]
Fe_3C/C-800	1.05 (*vs.* RHE)	0	0.83 (*vs.* RHE)	0	[41]
PMF-800	-	-	-	49	[43]
Fe_3C-Fe,N/C-900	-	-	0.881 (*vs.* RHE)	3	[45]
Fe_3C@NCNF-900	−0.035 (*vs.* SCE)	29	−0.121 (*vs.* SCE)	45	[46]
Fe/P/$C_{0.5}$-800	0.884 (*vs.* RHE)	−13	0.815 (*vs.* RHE)	6	[47]
Fe_3C/NCNF	1.012 (*vs.* RHE)	13	0.873 (*vs.* RHE)	46	[48]
Fe-N-CNFs	−0.02 (*vs.* Ag/AgCl)	−30	−0.140 (*vs.* Ag/AgCl)	−20	[49]
Fe_3C@C/rGO	-	-	0.95 (*vs.* RHE)	20	[53]
Fe_3C@N-CNT	-	-	0.85 (*vs.* RHE)	20	[54]
Fe_3C@C-900	-	-	0.80 (*vs.* RHE)	−20	[55]
Co_xP-CNTs-1000	−0.12 (*vs.* Ag/AgCl)	-	−0.20 (*vs.* Ag/AgCl)	20	[56]
CoP@SNC	-	-	0.81 (*vs.* RHE)	−70	[57]
Co_2P/N-HCR-2	0.962 (*vs.* RHE)	−19	0.811 (*vs.* RHE)	−19	[58]
Co_2P@CoNPG-900	0.90 (*vs.* RHE)	−10	0.81 (*vs.* RHE)	−10	[59]
NC@CoP_x/PyCNTs-900	0.92 (*vs.* RHE)	−10	-	-	[60]
FeP@NPCs	-	-	-	15	[61]
FeP@PNC-900	−0.054 (*vs.* Ag/AgCl)	13	−0.138 (*vs.* Ag/AgCl)	17	[62]
Fe_xP/NPCS	0.918 (*vs.* RHE)	−28	0.832 (*vs.* RHE)	4	[63]
α-Fe_2O_3/CNTs	−0.15 (*vs.* Ag/AgCl)	−50			[70]
Co_3O_4/NHPC	0.960 (*vs.* RHE)	4	0.835 (*vs.* RHE)	12	[72]
Fe_2O_3@Fe-N-C-800	0.054 (*vs.* Ag/AgCl)	−2	−0.104 (*vs.* Ag/AgCl)	32	[74]
Fe_9S_{10}(700)/N,S-G	0.959 (*vs.* RHE)	−38	0.800 (*vs.* RHE)	−13	[78]
Co_9S_8/NHCS-900	0.97 (*vs.* RHE)	−30	0.86 (*vs.* RHE)	10	[79]
($Fe_{1−x}$S/N,S-MGCS)$_{0.2}$	0.97 (*vs.* RHE)	40	0.91 (*vs.* RHE)	40	[81]
Lonogel-Fe-C-N	1.00 (*vs.* RHE)	0	0.87 (*vs.* RHE)	0	[82]
FeS/Fe_3C@N-S-C-800	-	-	0.87 (*vs.* RHE)	30	[85]
Fe-CZIF-800-10	0.982 (*vs.* RHE)	3	0.830 (*vs.* RHE)	4	[87]
Co@Co_3O_4@PPD	−0.1 (*vs.* Ag/AgCl)	−60	−0.17 (*vs.* Ag/AgCl)	−10	[89]
Fe-Fe_2O_3/NGr	0.075 (*vs.* Hg/HgO)	−15	−0.045 (*vs.* Hg/HgO)	−45	[90]
Co/Co_x@Co/N-graphene	−0.004 (*vs.* Hg/HgO)	−29	−0.125 (*vs.* Hg/HgO)	8	[91]

$\triangle E = E_{sample} − E_{Pt/C}$; RHE: reversible hydrogen electrode; SCE: saturated calomel electrode.

stability are the most concerned parameters. To improve the ORR activity in acidic media, it is meaningful to introduce other heteroatoms (B, P or S) to modify the charge distribution of the catalysts. Park et al. [39] synthesized a N,S-codoped carbon catalyst with graphitic carbon shells-coated Fe NPs by a hard-template method, and the catalyst was efficient for ORR in acidic media due to the synergistic effect between N,S-codoped carbon and the encapsulated Fe NPs. Compared with the encapsulated metal NPs in N-doped carbon layers mentioned above, this catalyst displayed a superior ORR performance in acidic media, indicating the high se-

Table 2 Comparision of ORR performances of Fe/Co-based NPs carbon catalysts in acidic media

Samples	E_{onset} (V)	$\triangle E_{onset}$ (mV)	$E_{1/2}$ (V)	$\triangle E_{1/2}$ (mV)	Ref.
Co@C-NCNTs	0.528 (*vs.* Ag/AgCl)	~60	-	-	[32]
Fe@NSC20-700$_1$-900$_1$	-	-	0.794 (*vs.* RHE)	−17	[39]
Fe$_3$C/C-700	0.90 (*vs.* RHE)	−100	0.73 (*vs.* RHE)	−100	[41]
PMF-800	0.886 (*vs.* RHE)	−44	-	-	[43]
Fe$_3$C-Fe,N/C-900	-	-	0.714 (*vs.* RHE)	−59	[45]
Fe$_3$C@NCNF-900	0.532 (*vs.* SCE)	−153	0.342 (*vs.* SCE)	−149	[46]
Fe/P/C$_{0.5}$-800	-	−56	-	−70	[47]
FeP@PNC-900	0.576 (*vs.* Ag/AgCl)	−58	0.487 (*vs.* Ag/AgCl)	−60	[62]
Fe$_x$P/NPCS	-	-	0.653 (*vs.* RHE)	−69	[63]
Fe$_2$O$_3$@Fe-N-C-800	0.698 (*vs.* Ag/AgCl)	−4	0.535 (*vs.* Ag/AgCl)	−34	[74]
Co$_9$S$_8$/NHCS-900	-	-	-	−76	[79]
(Fe$_{1−x}$S/N,S-MGCS)$_{0.2}$	0.81 (*vs.* RHE)	−90	0.73 (*vs.* RHE)	−80	[81]
FeS/Fe$_3$C@N-S-C-800	-	-	0.64 (*vs.* RHE)	−160	[85]

$\triangle E = E_{sample} − E_{Pt/C}$; RHE: reversible hydrogen electrode; SCE: saturated calomel electrode.
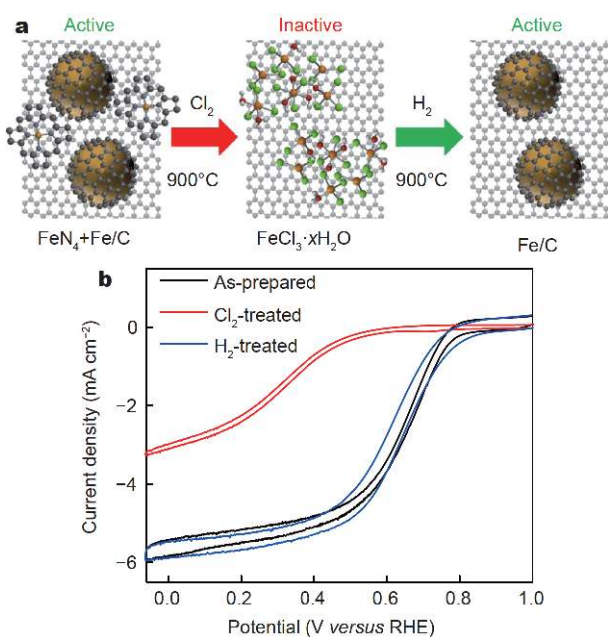
Figure 1 (a) Effect of Cl$_2$ and H$_2$ treatments on Fe species and ORR activity; (b) linear sweep voltammetry (LSV) curves of as-prepared, Cl$_2$-treated and H$_2$-treated catalysts in 0.1 mol L^{-1} HClO$_4$. Reprinted with permission from Ref. [28]. Copyright 2016, Nature Publishing Group.

lectivity toward 4e$^-$ reduction process of O$_2$. Therefore, introducing other heteroatoms into carbon matrix to regulate the structure of C-N sites was a feasible strategy to improve the ORR activity in acidic media. Moreover, in order to improve the stability of catalysts in harsh environment, some novel strategies were designed. For example, it was reported that a sandwich-like precursor,

which could introduce iron ions into a 2D C$_2$N matrix, was beneficial to obtaining catalyst with excellent durability [40].

MOFs were widely utilized to prepare carbon encapsulated Fe/Co metal catalysts. Most of these catalysts were highly efficient in alkaline media, and introducing sulfur into N-doped carbon matrix provided more active sites, resulting in effective catalysts in acidic media. However, it is still controversial whether Fe/Co-N moieties are effective for ORR.

Iron carbide NPs

Carbon encapsulated iron carbide NPs catalysts have been widely studied for ORR. A noteworthy publication which highlighted the importance of the encapsulated structure for iron carbide NPs was reported by Hu and co-workers [41]. Fe$_3$C/C catalysts were synthesized by a one-step high-pressure pyrolysis method with ferrocene and cyanamide as precursors. The catalyst possessed hollow spherical structure with a negligible amount of nitrogen or metal on the surface, and the Fe$_3$C NPs were encased by 4–9 graphitic layers. In alkaline media, Fe$_3$C/C-800 showed good activity comparable to the Pt/C catalyst. In acidic media, Fe$_3$C/C-700 exhibited relatively good values of onset and half-wave potentials, but ~100 mV lower than that of Pt/C. It displayed a low Tafel slope and a four-electron pathway dominated ORR process similar to Pt/C catalyst. Meanwhile, the catalyst exhibited excellent stability in acidic and alkaline media. It was proposed that although the NPs could not contact with the electrolyte directly, they played a vital role in
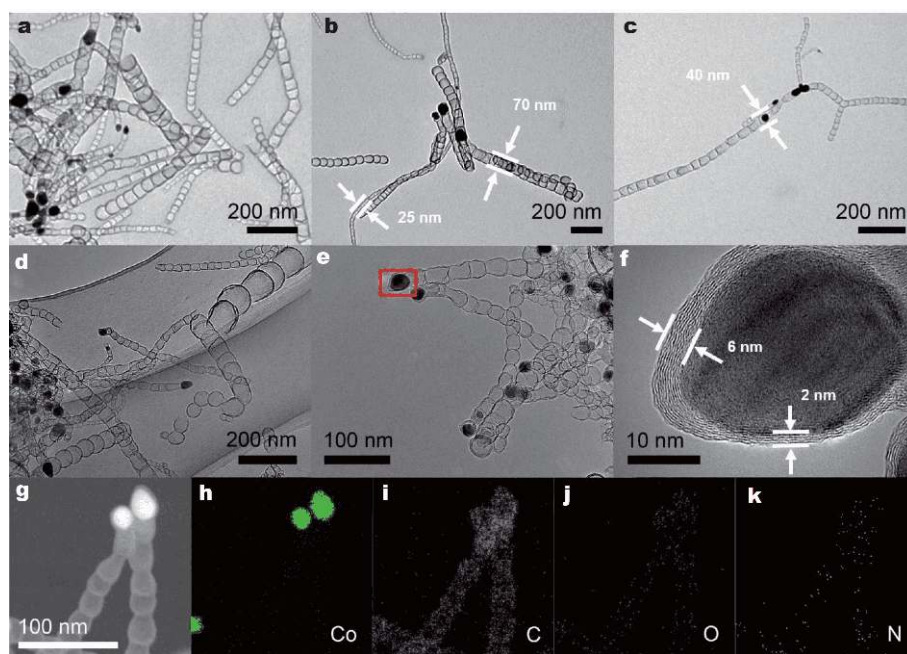
Figure 2 (a–e) Transmission electron microscopy (TEM) images, (f) high resolution TEM (HRTEM) image, (g–k) high-angle annular dark field scanning-TEM (HAADF/STEM) images and the corresponding energy dispersive X-ray spectroscopy (EDS) elemental mapping (Co, C, O, and N) of Co/N-BCNTs. Reprinted with permission from Ref. [33]. Copyright 2018, Royal Society of Chemistry.

activating the outer graphitic layers to catalyze the ORR process. In order to identify the effect of Fe_3C or Fe_2N particles on ORR activity, Sun *et al.* [42] designed Fe_3C- and Fe_2N-based catalysts with or without $Fe-N_x$ moieties in the carbon matrix. Based on experimental results, the high ORR activity was contributed by $Fe-N_x$ species instead of Fe_3C or Fe_2N. Meanwhile, DFT calculation results also demonstrated that the ORR activity of $Fe-N_x$ was much higher than that of Fe_3C or Fe_2N, consistent with the experimental results. Therefore, the effect of Fe_3C particles on ORR performance is still in dispute.

Other carbon-encapsulated iron carbide NP catalysts with different morphologies and structures were synthesized *via* hard or soft template methods [43–45]. By pyrolyzing the mixture of melamine, P123 and $Fe(NO_3)_3$, Yang and co-workers [43] reported a soft-template method to synthesize bamboo-like N-doped CNTs decorated with Fe_3C NPs. It was claimed that P123 played the role of soft template, assisting the 1D growth of carbon, and the catalyst exhibited a superior ORR activity and stability due to the unique structure. Liu *et al.* [44] developed a colloidal amphiphile-templating method to control the formation of Fe_3C nanocrystals encapsulated in mesoporous carbon nanospheres. Dopamine was applied to fabricate polymer nanospheres and ferric ions were absorbed into PDA nanospheres. The Fe-PDA na-

nospheres were pyrolyzed under N_2 atmosphere and then etched to remove the residual silica, and $Fe_3C@mCN$ was obtained with ultrafine Fe_3C NPs and mesoporous N-doped carbon nanospheres. Tan *et al.* [45] synthesized Fe_3C NPs encapsulated in iron-nitrogen-doped hollow carbon spheres by utilizing asymmetric triblock copolymer of poly(styrene-*b*-2-vinylpyridine-*b*-ethylene oxide) (PS-*b*-P2VP-*b*-PEO) as template. Melamine-formaldehyde resin (M-FR) was used as the source of carbon and nitrogen, and after annealing micelle@M-FR spheres mixed with $FeCl_3$, Fe_3C-Fe-N/C composed of Fe-N-doped carbon spheres decorated with encapsulated Fe_3C NPs was obtained. These examples revealed that the synergistic contribution of both composition and morphology resulted in the efficient ORR performance.

Electrospinning technique is a facile method which has been widely adopted to prepare heteroatom-doped carbon fibers with confined Fe_3C NPs [46–48]. Ren *et al.* [46] synthesized porous core-shell Fe_3C embedded N-doped carbon nanofibers *via* an electrospinning method. In alkaline media, the onset and half-wave potentials of the obtained catalyst were more positive than those of Pt/ C. However in acidic media, the ORR activity was unsatisfactory. Li and co-workers [47] introduced phosphorus into iron carbide-based catalyst and reported the synthesis of 3D hybrid carbon nanowires by carbonizing

the electrospun fiber [PVA/H$_3$PO$_4$/Fe(AC)$_2$] networks. The Fe/P/C nanowires catalyst displayed improved ORR activity in acidic media due to the abundant active sites (Fe$_3$C@C units, Fe–P and P–C bonds) and the hierarchically porous structure. Zhong et al. [48] introduced MOF (MIL-88B-NH$_2$) nanocrystals into poly(acrylonitrile) fibers by electrospinning method, and the obtained catalyst possessed abundant well-dispersed Fe$_3$C NPs and hierarchical pores, and exhibited improved ORR activity in acidic media. Therefore, abundant active sites and hierarchically porous structures are vital to further enhanced ORR activity. Addition of biomass carbonaceous fibers was another approach to obtain nanofiber catalysts [49,50]. By pyrolysis of polymer and iron ions on surface of carbonaceous nanofiber, Fe-N-doped carbon nanofibers with encapsulated Fe$_3$C NPs (Fe-N-CNFs) were obtained [49]. Instead of adsorbing iron ions, iron-tannin was applied as organic iron source to coat onto cellulose fibers, and this was beneficial to the formation of fine Fe$_3$C NPs coated with graphitic layers (Figs 3, 4), and the ORR performance of the catalyst was further enhanced [50].

Besides nanofibers, sheet-like carbon materials with coated iron carbide NPs were also efficient to catalyze oxygen reduction [51–53]. For instance, Jiang et al. [51] adopted a facile method to prepare Fe-N-doped carbon-sheets with Fe$_3$C NPs by annealing the mixture of urea, glucose and iron nitrate. Liu et al. [52] synthesized carbon nanosheets with encapsulated iron carbide by annealing low-cost precursors mixture (melamine, FeSO$_4$ and 1,10-phenanthroline). The obtained catalyst showed excellent ORR activity that outperformed Pt/C in alkaline media. Organic iron sources such as Fe-based MOFs and covalent organic polymers (COPs) were utilized to prepare carbon encapsulated iron carbide catalysts [54,55]. It was reported that a Fe-based MIL-88B guest was introduced into a Zn-based ZIF-8 host to form a MOF-in-MOF structure. This structure guaranteed in-situ confined pyrolysis of MIL-88B nanorods and facile synthesis of N-doped CNTs with small Fe$_3$C NPs. The pyrolysis process confined within the carbon matrix derived from organic ligands could effectively prevent the aggregation of formed Fe$_3$C NPs. Benefiting from the small size of these abundant Fe$_3$C and the hierarchically porous N-doped carbon structure, the as-prepared Fe$_3$C@N-doped CNTs exhibited a remarkable ORR activity in alkaline media [54]. Covalent porphyrin polymers (CPP) synthesized from terephthalaldehyde and pyrrole incorporated with iron chlorides (Fe-CPP) were converted into porous N-doped Fe$_3$C@Cs as reported by Kong et al. [55], and the
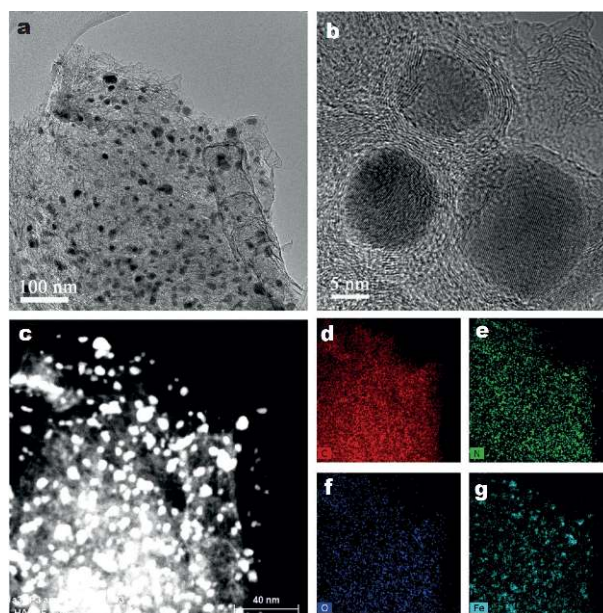

Figure 3 (a, b) TEM images of FP-Fe-TA-N-850; (c) STEM image of FP-Fe-TA-N-850, and its corresponding elements mapping images: C (d), N (e), O (f), Fe (g). Reprinted with permission from Ref. [50]. Copyright 2016, Wiley.

derived Fe$_3$C nanocrystals with 10–50 nm particle size were encapsulated in N-doped carbon shells.

For the fabrication of encapsulated iron carbide catalysts, specific organic iron sources facilitate the formation of fine NPs. Increasing the density of encapsulated iron carbide NPs and introducing phosphorus into the carbon matrix to modify catalyst structures would contribute to superior ORR activity. In addition, hard or soft template methods could be adopted to synthesize hierarchically porous carbon materials which are favorable for mass transport and electron transfer.

Co/Fe phosphide NPs
Transition metal phosphide-based carbon materials have attracted considerable attention in water electrolysis (hydrogen and oxygen evolution reaction (HER/OER)). Recent studies proved that they also showed efficient ORR activity. Chen et al. [56] reported that electron interaction between embedded Co$_2$P NPs and surface heteroatom-doped carbon could strongly promote the ORR catalytic performance. Heteroatoms doping played an important role to break the electroneutrality of carbon and facilitated oxygen adsorption, and the electron donor Co$_2$P NPs further accelerated the process of oxygen reduction. Co$_2$P NPs decorated heteroatom-doped mesoporous CNTs were fabricated by annealing the mixture of
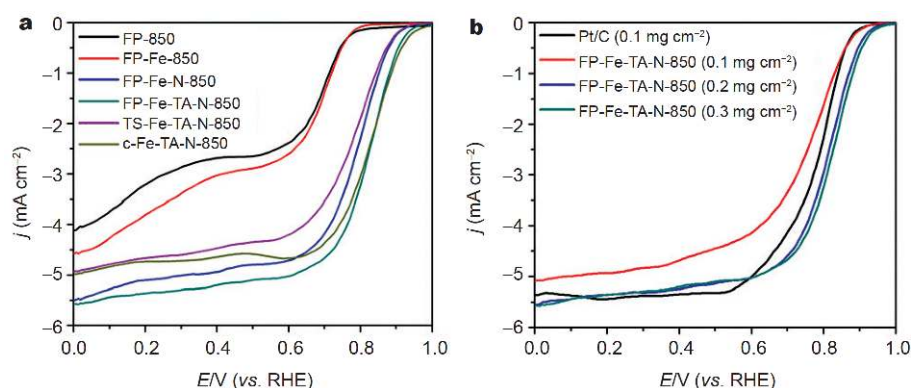
Figure 4 (a) LSV curves of prepared catalysts in 0.1 mol L^{-1} KOH; (b) LSV curves of Pt/C and FP-Fe-TA-N-850 with different loadings in 0.1 mol L^{-1} KOH. Reprinted with permission from Ref. [50]. Copyright 2016, Wiley.

cobaltous acetate and highly cross-linked organic-inorganic hybrid polymeric nanotubes [56]. Subsequently, several carbon catalysts with cobalt phosphide NPs were designed to improve ORR activity [57–59]. For example, Meng et al. [57] synthesized CoP quantum dots (QDs) embedded in S,N-codoped carbon, and the organophosphoric acid could strongly couple with Co^{2+} which ensured the small size of CoP during the annealing process. Wang et al. [58] synthesized hollow porous N-doped carbon rods with encapsulated Co$_2$P NPs via ball-milling. Jiang et al. [59] provided a supramolecular gel-assisted method to prevent the agglomeration of NPs and graphene embedded with Co$_2$P particles was obtained. It is unfortunate that the ORR activities of above-mentioned catalysts are still unable to surpass Pt/C catalyst in alkaline media. Wang et al. [60] developed a novel approach and synthesized hierarchically porous carbon tubes embedded with CoP$_x$ NPs, and this catalyst displayed an outstanding ORR performance and surpassed Pt/C catalyst (Figs 5, 6). In the study, pyridine-modified CNTs were mixed with melamine, phytic acid and porphyrin cobalt. For the obtained catalysts, CoP$_x$ NPs and CTNs were encapsulated in tubular carbon, and this hierarchically porous carbon matrix played an important role to improve the ORR activity, due to the excellent electron and mass transfer property.

According to the previous reports, Fe-based catalysts were usually more efficient than the Co-based ones. By using phytic acid and folic acid as phosphorus and nitrogen precursors, Zhang et al. [61] synthesized FeP NPs embedded in N,P dual-doped porous carbon nanosheets (FeP@NPCs). The N,P-codoped carbon nanosheets achieved more active sites than the single heteroatom doped ones, and the obtained mesoporous FeP@NPCs exhibited outstanding activity and durability toward both

ORR and OER in alkaline media. Xu et al. [62] synthesized iron phosphide NPs encapsulated into N,P-codoped carbon nanosheets by annealing low-cost precursors, and the catalyst exhibited efficient ORR catalytic activity and durability in both alkaline and acidic media. When the catalyst was treated to remove the FeP NPs, the ORR activity decreased observably. Therefore, it was proved that the synergistic effect between FeP NPs and heteroatom-doped carbon contributed to the remarkable ORR activity. Similarly, Hu et al. [63] synthesized Fe$_x$P/N,P-doped carbon nanosheets for ORR over the whole pH range, and they also proved that Fe$_x$P and N,P-doped carbon synergistically contributed to the high ORR performance.

Currently, the research of encapsulated Co/Fe phosphide NPs catalysts for ORR is insufficient and the activities are still undesirable. Phosphorus holds the similar valence electron structure with nitrogen, but it has stronger ability to donate electrons due to larger atomic radius and lower electronegativity than nitrogen. P-doped catalysts are expected to display efficient ORR performances, and the mechanism should be further explored to guide the development of highly efficient catalysts.

Fe/Co oxide NPs
Carbon materials with transition metal oxide NPs also played important roles in ORR [64]. Modified graphene oxide (GO), CNTs and other carbon substrates have been widely applied to improve mass transfer and electrical conductivity of the hybrid catalysts [65,66]. A significant study was reported by Liang and co-workers [67], in which Co$_3$O$_4$ NPs were grown on N-doped GO by a hydrothermal method. The hybrid catalyst showed high ORR performance, although Co$_3$O$_4$ itself exhibited little catalytic activities. Nitrogen doping in graphene further
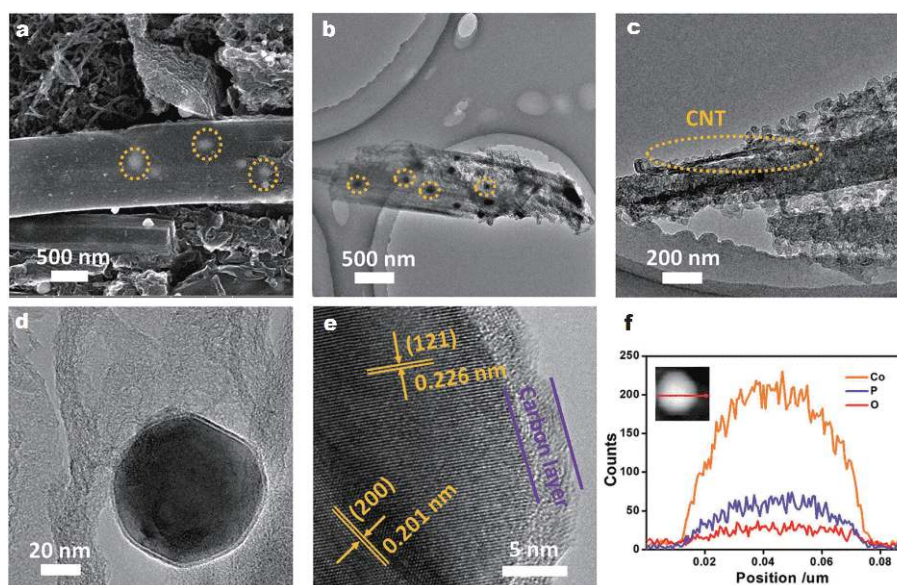
Figure 5 (a–e) Scanning electron microscopy (SEM) and TEM images of NC@CoP$_x$/PyCNTs-900; (f) line-scanning profile across a CoP$_x$ NP. Reprinted with permission from Ref. [60]. Copyright 2018, Elsevier.
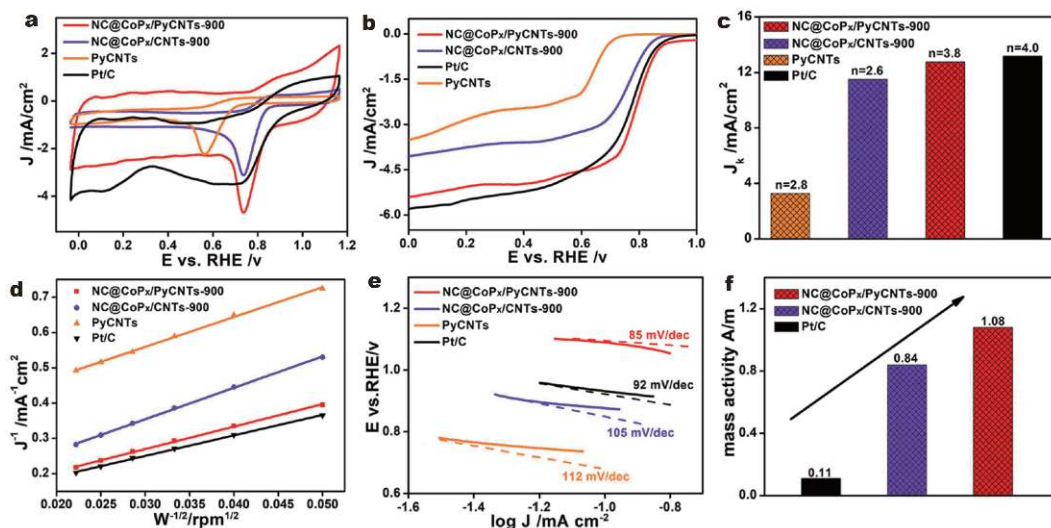
Figure 6 (a) Cyclic voltammetry (CV) and (b) LSV curves of prepared catalysts and Pt/C in 0.1 mol L^{-1} KOH; (c) electron transfer number and kinetic limiting current density (at 0.6 V); (d) Koutecky-Levich plots (at 0.6 V) of prepared catalysts and Pt/C; (e) Tafel plots derived from (b); (f) mass activity (at 0.75 V) of prepared catalysts and Pt/C. Reprinted with permission from Ref. [60]. Copyright 2018, Elsevier.

contributed to the improved ORR activity. This research provided a new idea for the fabrication of transition metal oxide electrocatalyst. Subsequently, Mao *et al.* [68] synthesized nitrogen-doped crumpled graphene (CG) balls with Co$_3$O$_4$ NPs, and the unique structure of CG maximized the surface area of the catalyst. Co$_3$O$_4$-CG balls were treated under ammonia atmosphere for nitrogen

doping, which was responsible for a low overpotential and a small Tafel slope. The as-prepared catalyst showed excellent ORR activity comparable to Pt/C in alkaline media. Besides GO, other porous carbon materials with different morphologies and structures were also suitable as substrates [69]. Carbon nanoweb (CNW) with 3D structure was prepared with cetrimonium bromide

(CTAB) and polypyrrole. Co_3O_4 or CNW alone displayed poor ORR activities, while the *in-situ* grown complex Co_3O_4-CNW had enhanced ORR performance, which provided strong evidence for the synergy of NPs and carbon supports. Similar results were found in iron oxide-based carbon catalysts [70]. Although the ORR activity was almost twice enhanced when α-Fe_2O_3 was attached to CNTs, it was still inferior to Pt/C. Doping nitrogen into carbon substrates or creating hierarchically porous carbon structures were effective strategies to improve ORR activities. Qiu and co-workers [71] adopted nitrogen-doped graphene to confine maghemite, and in the preparation process graphene was firstly modified with cyanamide, then ~2 nm sized γ-Fe_2O_3 NPs synthesized on N-doped graphene by hydrothermal reaction (Fig. 7). Due to the combined effect of highly dispersed NPs and porous carbon substrates, the as-prepared catalyst showed better ORR performance than commercial Pt/C in alkaline media. Guan *et al.* [72] adopted N-doped hierarchically porous carbon (NHPC) derived from cattle bone powder to confine Co_3O_4, and due to the large surface area, well-defined hierarchically porous structure and high nitrogen content of NHPC, Co_3O_4 with fine particle size was highly dispersed. As a result, the obtained Co_3O_4/NHPC exhibited efficient ORR and OER performances in alkaline media. The Zn-air battery adopted Co_3O_4/NHPC as the cathode catalyst showed superior performance with large specific capacity (795 mA h g_{Zn}^{-1} at 2 mA cm^{-2}) and high power density (80 mW cm^{-2}).

Different from the carbon encapsulated NPs catalysts, there were cases that no carbon-coating layers on the metal oxide NPs, and the bare oxide particles would suffer from dissolution or aggregation, leading to the decay of ORR activity. In order to resolve the durability issue, protection strategies were designed [73]. An active and stable catalyst Co_3O_4/CNT@C was prepared by annealing CNTs-Co_3O_4 hybrid coated with polydopamine. The catalyst displayed excellent long-term stability superior to Pt/C, and there was only 21 mV negative shift after 10,000 LSV test cycles. Meanwhile, the current density remained 83% after 100,000 s as evaluated by a chronoamperometric response. Xu *et al.* [74] fabricated a highly efficient Fe_2O_3@Fe-N-C electrocatalyst *via* a facile *in-situ* pyrolysis method, and Fe_2O_3 NPs covered with several graphitic carbon layers were encapsulated in carbon foams. In acidic media, the half-wave potential of Fe_2O_3@Fe-N-C was just 34 mV negative than that of Pt/C catalyst, and the relative current density remained 96.3% after 20,000 s.
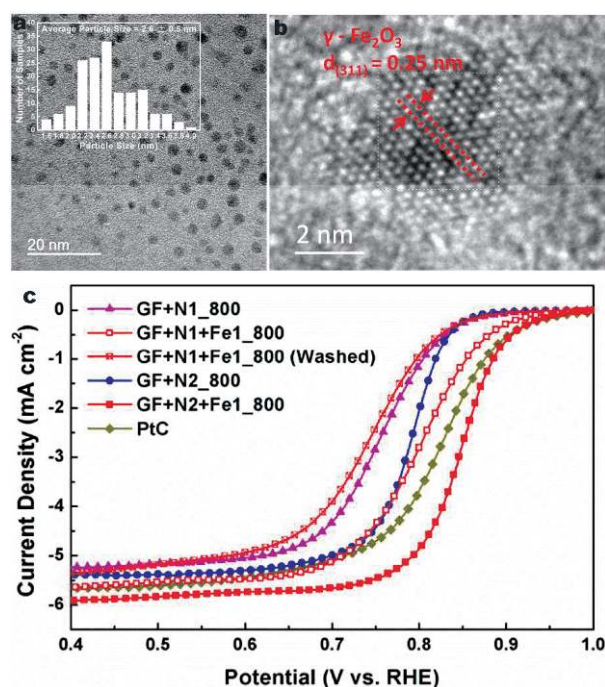
Figure 7 (a, b) TEM images of GF+N2+Fe1_800. The inset in (a) is the particle size distribution of γ-Fe_2O_3. (c) LSV curves of the prepared catalysts and Pt/C catalyst in 0.1 mol L^{-1} KOH. Reprinted with permission from Ref. [71]. Copyright 2016, American Chemical Society.

The combination of metal oxide and carbon substrates resulted in the improvement of ORR activity than that with metal oxide or carbon substrates alone. Compared with bare NPs embedded into carbon matrix, carbon encapsulated metal oxide catalysts displayed better ORR performance and long-term stability. Therefore, it is a feasible strategy to *in-situ* generate heteroatom-doped carbon encapsulated metal oxide NPs by annealing process.

Fe/Co sulfide NPs
Fe/Co sulfide-based carbon materials are another class of NPs/carbon catalysts for ORR. Generally, there are two main approaches for fabrication of metal sulfide decorated carbon catalysts: direct pyrolysis of precursors containing metal and sulfur elements or further sulfidization. Chen and co-workers [75] prepared N,S-codoped porous carbon with cobalt sulfide by a one-step carbonization and sulfurization approach, and hydrogen sulfide gas was introduced into argon gas flow during the annealing process. Luo and co-workers [76] synthesized CoS decorated N,S-codoped GO by using $Co(SCN)_2$ and GO as precursors. The crystal phase changed from Co_4S_3 to CoS *via* further sulfidization process, and the CoS

decorated catalyst showed a lower overpotential compared with other reported cobalt sulfide/carbon materials. A CoS$_2$/N,S-GO catalyst was prepared by direct pyrolysis of the GO and cobalt thiourea complex. Heteroatoms were doped into GO and CoS$_2$ NPs grew *in situ* on N,S-codoped GO concurrently [77]. Similarly, Fe$_9$S$_{10}$-decorated N,S-codoped GO was prepared with Fe,N,S-containing macrocycle compound and GO [78]. The ORR activities of above-mentioned catalysts were still not satisfactory. By annealing metanilic anions confined within cobalt-aluminum layered double hydroxides, the dispersity of Co$_9$S$_8$ NPs was improved, and the catalyst exhibited highly efficient ORR activity and stability in both alkaline and acidic media (shown in Figs 8, 9) [79]. Some polymers containing rich nitrogen were utilized as carbon sources, such as polypyrrole and polydopamine, which confined metal ions during the pyrolysis process [80,81]. Raisin bread-like N,S-codoped carbon spheres with iron sulfides NPs were prepared based on dopamine polymerization. The catalyst exhibited highly efficient ORR activity and stability in both alkaline and acidic media, and the reason could be ascribed to the high dispersity of Fe$_{1-x}$S NPs. Another direction to improve ORR activity is to construct hierarchically porous carbon substrates which are positive to mass transport and active sites exposure. Liu *et al.* [82] prepared hierarchically porous N,S-codoped carbon with FeS NPs, which showed efficient ORR activity outperforming that of Pt/C. However, a recently reported research showed that Fe$_{1-x}$S/S impaired the ORR activity [83]. Unexpectedly, a positive synergistic effect between Fe$_{1-x}$S/Fe$_3$O$_4$ and N,S-doped carbon greatly improved the ORR performance.

Currently, some studies revealed that Fe/Co sulfide NPs/carbon catalysts displayed efficient ORR activities due to the positive effect of Fe/Co sulfide; however some other studies claimed that metal sulfide had no ORR
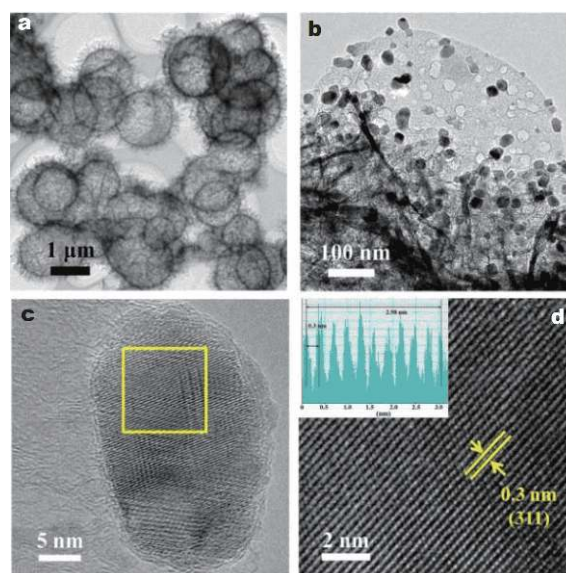

Figure 8 (a, b) TEM images and (c, d) HRTEM images of Co$_9$S$_8$/NHCS-900. Image (d) is the square region marked in (c). Reprinted with permission from Ref. [79]. Copyright 2016, Royal Society of Chemistry.

catalytic activity, or even impaired the activity. Therefore, the role of Fe/Co sulfide is still blurry and should be further explored.

Hybrid NPs

Hybrid NPs have also been reported to modify carbon [84–87]. S,N-doped carbon nanosheets encapsulated FeS/Fe$_3$C hybrid NPs were reported by Wei *et al.* [84], who adopted a glucose protective method to unroll and extend the wall of nanotubes. The authors proposed that FeS/Fe$_3$C hybrid NPs and the nanosheet structure synergistically contributed to the efficient ORR activity. Kong and co-workers [85] also prepared N,S-doped carbon with FeS/Fe$_3$C NPs by using a novel precursor. Firstly, COFs
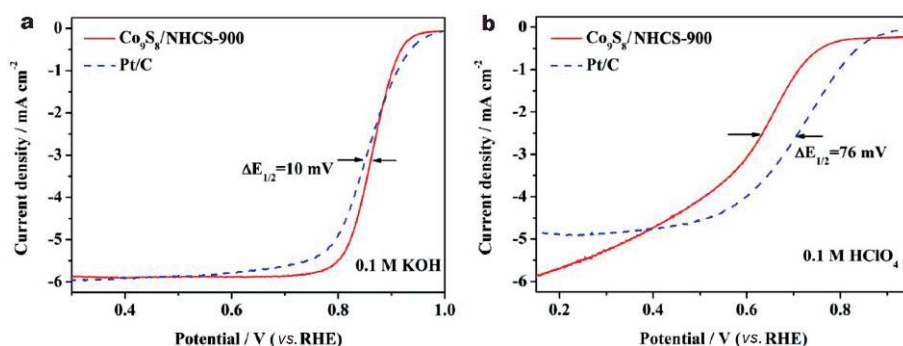
Figure 9 LSV curves of Co$_9$S$_8$/NHCS-900 and Pt/C in O$_2$-saturated (a) 0.1 mol L^{-1} KOH and (b) 0.1 mol L^{-1} HClO$_4$. Reprinted with permission from Ref. [79]. Copyright 2016, Royal Society of Chemistry.

polymers were synthesized *via* Suzuki coupling reaction, and then iron ions and dimethyl sulfoxide were absorbed into such polymers (Fe-Phen-COFs). After a pyrolysis process, the desired catalyst was obtained which displayed multiple electrocatalytic performances, and the enhanced activity was due to synergistic effect between the encapsulated FeS and Fe_3C. Additionally, heteroatom-doped carbon encapsulated Fe/Fe_3C hybrid NPs was reported efficient for ORR. A highly active Fe-N-C catalyst containing $Fe-N_x$ sites and Fe/Fe_3C NPs was prepared by pyrolyzing the mixture of glucose coated CNTs, iron salt and melamine. The authors proposed that due to the presence of Fe/Fe_3C NPs, $Fe–N_x$ sites were activated, and the ORR activity of catalyst was greatly promoted. Further results of DFT calculation showed this structure was beneficial to the adsorption of oxygen molecules [86]. Subsequently, N-doped flake-like carbon embedded with Fe/Fe_3C NPs was synthesized *via* annealing the mixture of ZIF-8 and potassium ferricyanide, and the hybrid NPs synergistically promoted ORR activity [87].

Metal/metal oxide NPs modified carbon catalysts also showed excellent ORR performance. Core-shell $Co@Co_3O_4$ NPs were rationally designed [88,89], and due

to the formation of a Schottky barrier between metal core and semiconductor shell, this core-shell structure was beneficial to charge separation, which was supposed to enhance ORR activity. It was reported that N-doped CNT-grafted carbon encapsulated $Co@Co_3O_4$ NPs was synthesized *via* two steps including annealing under H_2/He and O_2 atmosphere, and the as-prepared catalyst displayed highly efficient ORR/OER activity in alkaline media. Wang *et al.* [89] also synthesized catalysts with similar structure. Cobalt ions were confined in polydopamine *via* polymerization of dopamine (Figs 10, 11), and the obtained complex was annealed successively under N_2 and air atmosphere. Metal NPs treated under air atmosphere formed metal/metal oxide core-shell structure easily [90,91]. In addition, there was the case that metal particles formed together with oxide NPs inevitably during an annealing process.

Comparison of ORR performances of the Fe/Co based NPs catalysts

The ORR performances of the above-mentioned catalysts were summarized in Tables 1 and 2, in which onset and half-wave potentials were listed for comparison with Pt/C
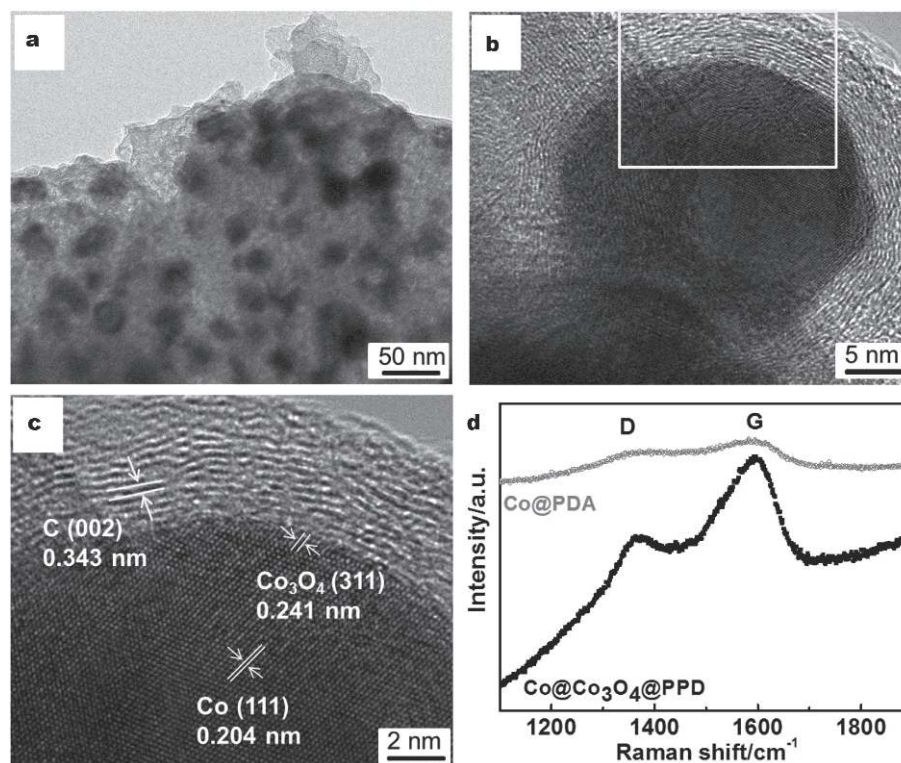
Figure 10 (a) TEM image of $Co@Co_3O_4@PPD$; (b, c) HRTEM image of $Co@Co_3O_4$ NP; (d) Raman spectra of Co@PDA and $Co@Co_3O_4@PPD$. Reprinted with permission from Ref. [89]. Copyright 2016, Wiley.
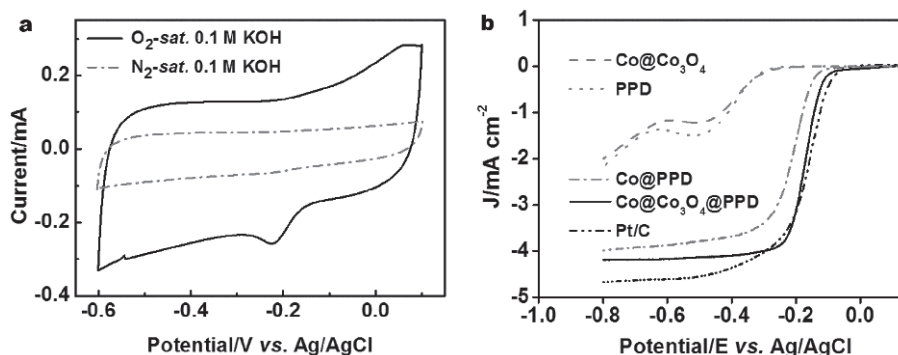
Figure 11 (a) CV curves of Co@Co$_3$O$_4$@PPD in O$_2$-saturated and N$_2$-saturated 0.1 mol L^{-1} KOH solution; (b) LSV curves of prepared catalysts and Pt/C catalyst in 0.1 mol L^{-1} KOH. Reprinted with permission from Ref. [89]. Copyright 2016, Wiley.

in alkaline and acidic media, respectively. Generally the ORR performances of metals and carbides NPs/carbon catalyst were superior to those of phosphides, oxides and sulfides, and Fe-based catalysts were more efficient than Co-based catalysts. Heteroatom doping, active sites density and carbon structures affected the catalytic activity greatly. Heteroatom-doping disturbed the electroneutrality of carbon and modified the charge distribution on carbon matrix, thus reduced the adsorption barrier of oxygen. N-doped catalysts were more efficient than the undoped ones and N,S/P-codoped catalysts were superior to the N-doped ones. Furthermore, a hierarchically porous carbon matrix was favorable to mass transport and electron transfer, which were crucial factors for ORR process.

According to Table 2, most of the listed catalysts did not exhibit high-efficiency in acidic media. The catalyst of doped carbon with Fe NPs prepared by a two-step pyrolysis process exhibited relatively good activity, due to the synergistic effect between the co-doping of S and N in the carbon matrix and the Fe NPs encapsulated in the doped carbon [35]. For the encapsulated NPs, the electrons would transfer from NPs to the coating heteroatom-doped carbon due to the synergistic effect; however the active sites located on the coating carbon matrix were mainly responsible for the ORR activity. The competitive formation of the Fe/Co based NPs would decrease the doping content of metal and heteroatoms in the carbon matrix, resulting in less active sites. Currently, Fe/N/S/C catalysts with abundant Fe-N$_x$ active sites have been reported efficient in acidic media, and it would be feasible to introduce abundant Fe-N$_x$ sites into carbon layers by multiple doping processes for better activity in acidic media.

SUMMARY AND OUTLOOK

The preparations, structural characterizations as well as ORR properties of a series of heteroatom-doped carbon with encapsulated or supported Fe/Co based NPs are briefly summarized including Fe/Co metals, carbides, phosphides, oxides, sulfides and hybrid NPs. These catalysts are generally synthesized by pyrolysis of precursors containing C, N, P, S and Fe/Co, or may be followed by further phosphorization/oxidization/sulfuration treatment. The precursors vary from small molecule substances to polymers, MOFs, COFs and so on. In addition, GO, CNTs or carbonaceous nanofibers could also be added to improve the electrical conductivity. Some strategies are applied to increase the dispersion of NPs and strengthen the bonding between particles and carbon supports, such as polymerization, ball milling, hydrothermal method and so on. Carbon materials with hierarchically porous structures are synthesized by hard or soft template methods. Although many efforts have been made to prepare Fe/Co based NPs/doped carbon catalysts, further exploration is still needed for the purpose of facile procedure, low cost and high ORR efficiency.

The ORR activities of catalysts in acidic media are significant for practical application, especially for polymer electrolyte membrane fuel cells (PEMFCs). Up to now, only a few catalysts are comparable to commercial Pt/C catalyst in acidic media, and it is a great challenge to develop highly efficient ORR catalysts in acidic media. For the encapsulated Fe/Co based NPs catalysts, the following strategies may be explored to enhance their performances in acidic media. i) As has been mentioned above, Fe/N/C catalysts with abundant Fe–N$_x$ active sites are efficient in acidic media. However, for the encapsulated NPs, the competitive formation of Fe/Co

based NPs would hinder the content of Fe/Co doping in the coating carbon, and thus would decrease the active sites on the coating carbon. To solve this problem, multiple-step doping methods should be adopted to increase the doping of Fe/Co, nitrogen, phosphors or sulfur into the coating carbon matrix. ii) The synergistic effect between the encapsulated Fe/Co based NPs and the doped carbon is the key point in ORR for the encapsulated Fe/Co based NPs catalysts. Further increasing the loading or decreasing the size of NPs, or decreasing the layers of the coating carbon would create more interface, and thus would enhance the synergistic effect, and new precursors as well as new pyrolysis processes would be expected to achieve those control conditions. iii) Certain encapsulated hybrid-NPs composed of different types of nanocrystals may improve the electron transfer effect on coating carbon, and it would be possible to employ specific functional molecules into precursors to obtain hybrid-NPs encapsulated in carbon. Compared with single type of NPs, the hybrid-NPs may exhibit unique synergistic effect to design heteroatom-doped carbon matrix and thus induce excellent ORR performance.

There should be further mechanism research on atomic or molecular level in the future, because the true active sites for ORR are still vague at present. Although it has been proved that the synergistic effects between Fe/Co based NPs and carbon substrates improve ORR activity experimentally, the molecular level mechanism is not exactly clear. A precise mechanism can provide a right direction for design and synthesis of efficient catalysts. In-situ characterizations and theoretic calculations are greatly encouraged and the research results would provide a deep insight into the mechanism.

1 Dai L, Xue Y, Qu L, et al. Metal-free catalysts for oxygen reduction reaction. Chem Rev, 2015, 115: 4823–4892

2 Qu K, Zheng Y, Dai S, et al. Graphene oxide-polydopamine derived N, S-codoped carbon nanosheets as superior bifunctional electrocatalysts for oxygen reduction and evolution. Nano Energy, 2016, 19: 373–381

3 Wang YJ, Zhao N, Fang B, et al. Carbon-supported Pt-based alloy electrocatalysts for the oxygen reduction reaction in polymer electrolyte membrane fuel cells: Particle size, shape, and composition manipulation and their impact to activity. Chem Rev, 2015, 115: 3433–3467

4 Jiao Y, Zheng Y, Jaroniec M, et al. Design of electrocatalysts for oxygen- and hydrogen-involving energy conversion reactions. Chem Soc Rev, 2015, 44: 2060–2086

5 Fujimoto S, Mizuno R, Saito Y, et al. Clinical application of wave intensity for the treatment of essential hypertension. Heart Vessels, 2004, 19: 19–22

6 Wang DW, Su D. Heterogeneous nanocarbon materials for oxygen reduction reaction. Energy Environ Sci, 2014, 7: 576

7 Zhang G, Jia Y, Zhang C, et al. A general route via formamide condensation to prepare atomically dispersed metal–nitrogen–carbon electrocatalysts for energy technologies. Energy Environ Sci, 2019, 12: 1317–1325

8 Zhu YP, Qiao SZ. Unprecedented carbon sub-microspheres with a porous hierarchy for highly efficient oxygen electrochemistry. Nanoscale, 2017, 9: 18731–18736

9 Cheng Y, He S, Lu S, et al. Iron single atoms on graphene as nonprecious metal catalysts for high-temperature polymer electrolyte membrane fuel cells. Adv Sci, 2019, 6: 1802066

10 Liu YL, Shi CX, Xu XY, et al. Nitrogen-doped hierarchically porous carbon spheres as efficient metal-free electrocatalysts for an oxygen reduction reaction. J Power Sources, 2015, 283: 389–396

11 Liu L, Zhang J, Ma W, et al. Co/N co-doped graphene-like nanocarbon for highly efficient oxygen reduction electrocatalyst. Sci China Mater, 2018, 62: 359–367

12 Yan D, Guo L, Xie C, et al. N, P-dual doped carbon with trace Co and rich edge sites as highly efficient electrocatalyst for oxygen reduction reaction. Sci China Mater, 2017, 61: 679–685

13 Chen P, Zhou T, Xing L, et al. Atomically dispersed iron-nitrogen species as electrocatalysts for bifunctional oxygen evolution and reduction reactions. Angew Chem Int Ed, 2017, 56: 610–614

14 Shen H, Gracia-Espino E, Ma J, et al. Synergistic effects between atomically dispersed Fe−N−C and C−S−C for the oxygen reduction reaction in acidic media. Angew Chem Int Ed, 2017, 56: 13800–13804

15 Li Q, Chen W, Xiao H, et al. Fe isolated single atoms on S, N codoped carbon by copolymer pyrolysis strategy for highly efficient oxygen reduction reaction. Adv Mater, 2018, 30: 1800588

16 Liang J, Jiao Y, Jaroniec M, et al. Sulfur and nitrogen dual-doped mesoporous graphene electrocatalyst for oxygen reduction with synergistically enhanced performance. Angew Chem Int Ed, 2012, 51: 11496–11500

17 Sun T, Wang J, Qiu C, et al. B, N codoped and defect-rich nanocarbon material as a metal-free bifunctional electrocatalyst for oxygen reduction and evolution reactions. Adv Sci, 2018, 5: 1800036

18 Wang XR, Liu JY, Liu ZW, et al. Identifying the key role of pyridinic-N-Co bonding in synergistic electrocatalysis for reversible ORR/OER. Adv Mater, 2018, 30: 1800005

19 Fan X, Kong F, Kong A, et al. Covalent porphyrin framework-derived $Fe_2P@Fe_4N$-coupled nanoparticles embedded in N-doped carbons as efficient trifunctional electrocatalysts. ACS Appl Mater Interfaces, 2017, 9: 32840–32850

20 Zhao H, Yuan ZY. Transition metal–phosphorus-based materials for electrocatalytic energy conversion reactions. Catal Sci Technol, 2017, 7: 330–347

21 Ren Q, Wang H, Lu XF, et al. Recent progress on MOF-derived heteroatom-doped carbon-based electrocatalysts for oxygen reduction reaction. Adv Sci, 2018, 5: 1700515

22 Wang T, Wang J, Wang X, et al. Graphene-templated synthesis of sandwich-like porous carbon nanosheets for efficient oxygen reduction reaction in both alkaline and acidic media. Sci China Mater, 2018, 61: 915–925

23 Li C, Zhao J, Priestley RD, et al. Constrained-volume assembly of organometal confined in polymer to fabricate multi-heteroatom

doped carbon for oxygen reduction reaction. Sci China Mater, 2018, 61: 1305–1313

24 Wu G, More KL, Johnston CM, et al. High-performance electrocatalysts for oxygen reduction derived from polyaniline, iron, and cobalt. Science, 2011, 332: 443–447

25 Deng D, Yu L, Chen X, et al. Iron encapsulated within pod-like carbon nanotubes for oxygen reduction reaction. Angew Chem Int Ed, 2013, 52: 371–375

26 Liang HW, Zhuang X, Brüller S, et al. Hierarchically porous carbons with optimized nitrogen doping as highly active electrocatalysts for oxygen reduction. Nat Commun, 2014, 5: 4973

27 Wei W, Liang H, Parvez K, et al. Nitrogen-doped carbon nanosheets with size-defined mesopores as highly efficient metal-free catalyst for the oxygen reduction reaction. Angew Chem Int Ed, 2014, 53: 1570–1574

28 Varnell JA, Tse ECM, Schulz CE, et al. Identification of carbon-encapsulated iron nanoparticles as active species in non-precious metal oxygen reduction catalysts. Nat Commun, 2016, 7: 12582

29 Strickland K, Miner E, Jia Q, et al. Highly active oxygen reduction non-platinum group metal electrocatalyst without direct metal–nitrogen coordination. Nat Commun, 2015, 6: 7343

30 Mao C, Kong A, Wang Y, et al. MIL-100 derived nitrogen-embodied carbon shells embedded with iron nanoparticles. Nanoscale, 2015, 7: 10817–10822

31 Dou S, Li X, Tao L, et al. Cobalt nanoparticle-embedded carbon nanotube/porous carbon hybrid derived from MOF-encapsulated Co₃O₄ for oxygen electrocatalysis. Chem Commun, 2016, 52: 9727–9730

32 Li R, Wang X, Dong Y, et al. Nitrogen-doped carbon nanotubes decorated with cobalt nanoparticles derived from zeolitic imidazolate framework-67 for highly efficient oxygen reduction reaction electrocatalysis. Carbon, 2018, 132: 580–588

33 Wang R, Yan T, Han L, et al. Tuning the dimensions and structures of nitrogen-doped carbon nanomaterials derived from sacrificial g-C₃N₄/metal–organic frameworks for enhanced electrocatalytic oxygen reduction. J Mater Chem A, 2018, 6: 5752–5761

34 Hu E, Ning J, He B, et al. Unusual formation of tetragonal microstructures from nitrogen-doped carbon nanocapsules with cobalt nanocores as a bi-functional oxygen electrocatalyst. J Mater Chem A, 2017, 5: 2271–2279

35 Zhang X, Lin J, Chen S, et al. Co nanoparticles encapsulated in N-doped carbon nanosheets: Enhancing oxygen reduction catalysis without metal–nitrogen bonding. ACS Appl Mater Interfaces, 2017, 9: 38499–38506

36 Zeng M, Liu Y, Zhao F, et al. Metallic cobalt nanoparticles encapsulated in nitrogen-enriched graphene shells: Its bifunctional electrocatalysis and application in zinc-air batteries. Adv Funct Mater, 2016, 26: 4397–4404

37 Li C, Wu M, Liu R. High-performance bifunctional oxygen electrocatalysts for zinc-air batteries over mesoporous Fe/Co-N-C nanofibers with embedding FeCo alloy nanoparticles. Appl Catal B-Environ, 2019, 244: 150–158

38 Wu N, Lei Y, Wang Q, et al. Facile synthesis of FeCo@NC core–shell nanospheres supported on graphene as an efficient bifunctional oxygen electrocatalyst. Nano Res, 2017, 10: 2332–2343

39 Park HS, Han SB, Kwak DH, et al. Fe nanoparticles encapsulated in doped graphitic shells as high-performance and stable catalysts for oxygen reduction reaction in an acid medium. J Catal, 2019, 370: 130–137

40 Mahmood J, Li F, Kim C, et al. Fe@C₂N: A highly-efficient indirect-contact oxygen reduction catalyst. Nano Energy, 2018, 44: 304–310

41 Hu Y, Jensen JO, Zhang W, et al. Hollow spheres of iron carbide nanoparticles encased in graphitic layers as oxygen reduction catalysts. Angew Chem Int Ed, 2014, 53: 3675–3679

42 Sun T, Jiang Y, Wu Q, et al. Is iron nitride or carbide highly active for oxygen reduction reaction in acidic medium? Catal Sci Technol, 2017, 7: 51–55

43 Yang W, Liu X, Yue X, et al. Bamboo-like carbon nanotube/Fe₃C nanoparticle hybrids and their highly efficient catalysis for oxygen reduction. J Am Chem Soc, 2015, 137: 1436–1439

44 Liu B, Yao H, Daniels RA, et al. A facile synthesis of Fe₃C@mesoporous carbon nitride nanospheres with superior electrocatalytic activity. Nanoscale, 2016, 8: 5441–5445

45 Tan H, Li Y, Kim J, et al. Sub-50 nm iron-nitrogen-doped hollow carbon sphere-encapsulated iron carbide nanoparticles as efficient oxygen reduction catalysts. Adv Sci, 2018, 5: 1800120

46 Ren G, Lu X, Li Y, et al. Porous core–shell Fe₃C embedded N-doped carbon nanofibers as an effective electrocatalysts for oxygen reduction reaction. ACS Appl Mater Interfaces, 2016, 8: 4118–4125

47 Li M, Liu T, Bo X, et al. Hybrid carbon nanowire networks with Fe–P bond active site for efficient oxygen/hydrogen-based electrocatalysis. Nano Energy, 2017, 33: 221–228

48 Zhong R, Wu Y, Liang Z, et al. Fabricating hierarchically porous and Fe₃C-embeded nitrogen-rich carbon nanofibers as exceptional electocatalysts for oxygen reduction. Carbon, 2019, 142: 115–122

49 Wu ZY, Xu XX, Hu BC, et al. Iron carbide nanoparticles encapsulated in mesoporous Fe-N-doped carbon nanofibers for efficient electrocatalysis. Angew Chem Int Ed, 2015, 54: 8179–8183

50 Wei J, Liang Y, Hu Y, et al. A versatile iron-tannin-framework ink coating strategy to fabricate biomass-derived iron carbide/Fe-N-carbon catalysts for efficient oxygen reduction. Angew Chem Int Ed, 2016, 55: 1355–1359

51 Jiang H, Yao Y, Zhu Y, et al. Iron carbide nanoparticles encapsulated in mesoporous Fe–N-doped graphene-like carbon hybrids as efficient bifunctional oxygen electrocatalysts. ACS Appl Mater Interfaces, 2015, 7: 21511–21520

52 Liu YL, Xu XY, Sun PC, et al. N-doped porous carbon nanosheets with embedded iron carbide nanoparticles for oxygen reduction reaction in acidic media. Int J Hydrogen Energy, 2015, 40: 4531–4539

53 Li J, Mao S, Hou Y, et al. 3D edge-enriched Fe₃C@C nanocrystals with a core-shell structure grown on reduced graphene oxide networks for efficient oxygen reduction reaction. ChemSusChem, 2018, 11: 3292–3298

54 Guan BY, Yu L, (David) Lou XW. A dual-metal–organic-framework derived electrocatalyst for oxygen reduction. Energy Environ Sci, 2016, 9: 3092–3096

55 Kong A, Zhang Y, Chen Z, et al. One-pot synthesized covalent porphyrin polymer-derived core-shell Fe₃C@carbon for efficient oxygen electroreduction. Carbon, 2017, 116: 606–614

56 Chen K, Huang X, Wan C, et al. Efficient oxygen reduction catalysts formed of cobalt phosphide nanoparticle decorated heteroatom-doped mesoporous carbon nanotubes. Chem Commun, 2015, 51: 7891–7894

57 Meng T, Hao YN, Zheng L, et al. Organophosphoric acid-derived CoP quantum dots@S,N-codoped graphite carbon as a trifunctional electrocatalyst for overall water splitting and Zn–air batteries. Nanoscale, 2018, 10: 14613–14626

58 Wang H, Wang W, Xu YY, *et al.* Ball-milling synthesis of Co_2P nanoparticles encapsulated in nitrogen doped hollow carbon rods as efficient electrocatalysts. J Mater Chem A, 2017, 5: 17563–17569

59 Jiang H, Li C, Shen H, *et al.* Supramolecular gel-assisted synthesis Co_2P particles anchored in multielement co-doped graphene as efficient bifunctional electrocatalysts for oxygen reduction and evolution. Electrochim Acta, 2017, 231: 344–353

60 Wang Q, Fan Y, Wang K, *et al.* Hierarchical tubular structures composed of CoP_x and carbon nanotubes: Highly effective electrocatalyst for oxygen reduction. Carbon, 2018, 130: 241–249

61 Zhang R, Zhang C, Chen W. FeP embedded in N, P dual-doped porous carbon nanosheets: An efficient and durable bifunctional catalyst for oxygen reduction and evolution reactions. J Mater Chem A, 2016, 4: 18723–18729

62 Xu X, Shi C, Chen R, *et al.* Iron phosphide nanocrystals decorated in situ on heteroatom-doped mesoporous carbon nanosheets used for an efficient oxygen reduction reaction in both alkaline and acidic media. RSC Adv, 2017, 7: 22263–22269

63 Hu K, Xiao Z, Cheng Y, *et al.* Iron phosphide/N, P-doped carbon nanosheets as highly efficient electrocatalysts for oxygen reduction reaction over the whole pH range. Electrochim Acta, 2017, 254: 280–286

64 Ishihara A, Ohgi Y, Matsuzawa K, *et al.* Progress in non-precious metal oxide-based cathode for polymer electrolyte fuel cells. Electrochim Acta, 2010, 55: 8005–8012

65 Zhang G, Xu Y, Wang L, *et al.* Rational design of graphene oxide and its hollow CoO composite for superior oxygen reduction reaction. Sci China Mater, 2015, 58: 534–542

66 Sun M, Zhang G, Liu H, *et al.* α- and γ-Fe_2O_3 nanoparticle/nitrogen doped carbon nanotube catalysts for high-performance oxygen reduction reaction. Sci China Mater, 2015, 58: 683–692

67 Liang Y, Li Y, Wang H, *et al.* Co_3O_4 nanocrystals on graphene as a synergistic catalyst for oxygen reduction reaction. Nat Mater, 2011, 10: 780–786

68 Mao S, Wen Z, Huang T, *et al.* High-performance bi-functional electrocatalysts of 3D crumpled graphene–cobalt oxide nanohybrids for oxygen reduction and evolution reactions. Energy Environ Sci, 2014, 7: 609–616

69 Liu S, Li L, Ahn HS, *et al.* Delineating the roles of Co_3O_4 and N-doped carbon nanoweb (CNW) in bifunctional Co_3O_4/CNW catalysts for oxygen reduction and oxygen evolution reactions. J Mater Chem A, 2015, 3: 11615–11623

70 Sun M, Dong Y, Zhang G, *et al.* α-Fe_2O_3 spherical nanocrystals supported on CNTs as efficient non-noble electrocatalysts for the oxygen reduction reaction. J Mater Chem A, 2014, 2: 13635–13640

71 Qiu K, Chai G, Jiang C, *et al.* Highly efficient oxygen reduction catalysts by rational synthesis of nanoconfined maghemite in a nitrogen-doped graphene framework. ACS Catal, 2016, 6: 3558–3568

72 Guan J, Zhang Z, Ji J, *et al.* Hydrothermal synthesis of highly dispersed Co_3O_4 nanoparticles on biomass-derived nitrogen-doped hierarchically porous carbon networks as an efficient bifunctional electrocatalyst for oxygen reduction and evolution reactions. ACS Appl Mater Interfaces, 2017, 9: 30662–30669

73 Yang F, Abadia M, Chen C, *et al.* Design of active and stable oxygen reduction reaction catalysts by embedding Co_xO_y nanoparticles into nitrogen-doped carbon. Nano Res, 2016, 10: 97–107

74 Xu X, Shi C, Li Q, *et al.* Fe–N-doped carbon foam nanosheets with embedded Fe_2O_3 nanoparticles for highly efficient oxygen reduction in both alkaline and acidic media. RSC Adv, 2017, 7: 14382–14388

75 Chen B, Li R, Ma G, *et al.* Cobalt sulfide/N,S codoped porous carbon core–shell nanocomposites as superior bifunctional electrocatalysts for oxygen reduction and evolution reactions. Nanoscale, 2015, 7: 20674–20684

76 Luo Z, Tan C, Zhang X, *et al.* Preparation of cobalt sulfide nanoparticle-decorated nitrogen and sulfur co-doped reduced graphene oxide aerogel used as a highly efficient electrocatalyst for oxygen reduction reaction. Small, 2016, 12: 5920–5926

77 Ganesan P, Prabu M, Sanetuntikul J, *et al.* Cobalt sulfide nanoparticles grown on nitrogen and sulfur codoped graphene oxide: An efficient electrocatalyst for oxygen reduction and evolution reactions. ACS Catal, 2015, 5: 3625–3637

78 Ma XX, Su Y, He XQ. Fe_9S_{10}-decorated N, S co-doped graphene as a new and efficient electrocatalyst for oxygen reduction and oxygen evolution reactions. Catal Sci Technol, 2017, 7: 1181–1192

79 Wang J, Li L, Chen X, *et al.* Monodisperse cobalt sulfides embedded within nitrogen-doped carbon nanoflakes: An efficient and stable electrocatalyst for the oxygen reduction reaction. J Mater Chem A, 2016, 4: 11342–11350

80 Lin L, Qin H, Jia J, *et al.* FeS as a promising cathode catalyst for direct borohydride fuel cells. J Alloys Compd, 2018, 769: 136–140

81 Xiao J, Xia Y, Hu C, *et al.* Raisin bread-like iron sulfides/nitrogen and sulfur dual-doped mesoporous graphitic carbon spheres: A promising electrocatalyst for the oxygen reduction reaction in alkaline and acidic media. J Mater Chem A, 2017, 5: 11114–11123

82 Liu S, Yang Z, Li M, *et al.* FeS-decorated hierarchical porous N, S-dual-doped carbon derived from silica-ionogel as an efficient catalyst for oxygen reduction reaction in alkaline media. Electrochim Acta, 2018, 265: 221–231

83 Zhang J, Xu D, Wang C, *et al.* Rational design of $Fe_{1-x}S$/Fe_3O_4/ nitrogen and sulfur-doped porous carbon with enhanced oxygen reduction reaction catalytic activity. Adv Mater Interfaces, 2018, 5: 1701641

84 Wei C, Shen M, Ai K, *et al.* Transformation from FeS/Fe_3C nanoparticles encased S, N dual doped carbon nanotubes to nanosheets for enhanced oxygen reduction performance. Carbon, 2017, 123: 135–144

85 Kong F, Fan X, Kong A, *et al.* Covalent phenanthroline framework derived FeS@Fe_3C composite nanoparticles embedding in N-S-codoped carbons as highly efficient trifunctional electrocatalysts. Adv Funct Mater, 2018, 28: 1803973

86 Jiang WJ, Gu L, Li L, *et al.* Understanding the high activity of Fe–N–C electrocatalysts in oxygen reduction: Fe/Fe_3C nanoparticles boost the activity of Fe–N_x. J Am Chem Soc, 2016, 138: 3570–3578

87 Li G, Zhang J, Li W, *et al.* 3D interconnected hierarchical porous N-doped carbon constructed by flake-like nanostructure with Fe/Fe_3C for efficient oxygen reduction reaction and supercapacitor. Nanoscale, 2018, 10: 9252–9260

88 Aijaz A, Masa J, Rösler C, *et al.* Co@Co_3O_4 encapsulated in carbon nanotube-grafted nitrogen-doped carbon polyhedra as an advanced bifunctional oxygen electrode. Angew Chem Int Ed, 2016, 55: 4087–4091

89 Wang Z, Li B, Ge X, *et al.* Co@Co_3O_4@PPD core@bishell nanoparticle-based composite as an efficient electrocatalyst for oxygen reduction reaction. Small, 2016, 12: 2580–2587

90 Dhavale VM, Singh SK, Nadeema A, *et al.* Nanocrystalline Fe–Fe_2O_3 particle-deposited N-doped graphene as an activity-modulated Pt-free electrocatalyst for oxygen reduction reaction. Nanoscale, 2015, 7: 20117–20125

91   Niu Y, Huang X, Wu X, *et al.* One-pot synthesis of Co/N-doped mesoporous graphene with embedded Co/CoO$_x$ nanoparticles for efficient oxygen reduction reaction. Nanoscale, 2017, 9: 10233–10239

Author contributions   Ni B and Chen T designed the outlines; Ni B, Wu L, Chen R and Shi C collected the literature and wrote the paper.

Conflict of interest   The authors declare that they have no conflict of interest.

Baoxia Ni is currently a PhD student under the supervision of Prof. Tiehong Chen, at the School of Materials Science and Engineering, Nankai University. Her research focuses on the design and synthesis of nanostructured carbon electrocatalysts.

Tiehong Chen received his BSc and PhD degrees from Nankai University in 1990 and 1996, respectively. He joined Nankai University in 1996 and is currently a professor at the School of Materials Science and Engineering. His current research interests include heterogeneous catalysis, electrocatalysis and synthesis of zeolites and mesoporous materials.

掺杂碳封装的Fe/Co基纳米颗粒氧还原催化剂

倪保霞，武鲁明，陈睿，史成香，陈铁红[*]

摘要   氧还原反应是电化学能量转换和存储装置的重要反应过程，但其反应动力学缓慢，因此开发高效低成本的氧还原催化剂至关重要. 目前，包裹过渡金属基纳米颗粒的碳材料因其优异的氧还原催化活性，引起了广泛关注. 本文按照金属基纳米颗粒的类别从金属、碳化物、磷化物、氧化物、硫化物以及混合颗粒等六个方面综述了掺杂碳封装的Fe/Co基纳米颗粒氧还原催化剂. 催化剂碳基质的结构、纳米颗粒的种类及其分布对催化性能有很大影响，目前这类催化剂在碱性介质中表现出了优异的氧还原活性和稳定性，但在酸性介质中的活性仍需要进一步提高. 文章讨论了制备封装型纳米颗粒/碳高效氧还原催化剂过程中存在的挑战，并展望了其发展前景.